RSC Advances

ROYAL SOCIETY OF CHEMISTRY

www.rsc.org/advances

Journal Name

ARTICLE

Microbial preparation of magnetite/reduced graphene oxide nanocomposite for removal of organic dyes from aqueous solutions

Guangfei Liu,[a, b] Ning Wang,[a] Jiti Zhou,[*a] Aijie Wang,[*b] Jing Wang,[a] Ruofei Jin,[a] Hong Lv[a]

Received 00th January 20xx,
Accepted 00th January 20xx

DOI: 10.1039/x0xx00000x

www.rsc.org/

Magnetic graphene materials are good adsorbents for pollutants removal from aqueous solutions. However, most chemical methods for the synthesis of magnetic adsorbents generally require the use of toxic reductants, proceed under rigorous conditions, and thus cause negative impacts on the environment. Here, an eco-friendly method applying the reduction activity of microbial cells was developed to prepare magnetite/reduced graphene oxide (MRGO) nanocomposite for adsorptive removal of organic dyes. The biogenic MRGO was characterized by transmission electron microscopy, X-ray diffraction, Fourier transform infrared spectroscopy, X-ray photoelectron spectroscopy and vibrating sample magnetometer. Factors (adsorbent dosage, contact time, solution pH and ionic strength, etc.) affecting the adsorption process were investigated. The adsorption behavior of MRGO fits well with Langmuir isotherm and pseudo-second-order kinetic model. The maximum adsorption capacity of MRGO for methylene blue at 303 K was determined to be 144.9 mg g^{-1}, which is higher than those of many other chemically synthesized magnetic graphene materials. Thermodynamic analysis revealed the spontaneous and endothermic nature of the adsorption process. Moreover, the MRGO adsorbent could be regenerated through a Fenton-like reaction and reused effectively in five successive runs. The biogenic MRGO has great potentials for the treatment of wastewater containing dyes and other environmental pollutants.

Introduction

A variety of organic dyes have been extensively used in many different fields, such as printing, textile, dyeing, paper and pulp, cosmetic, pharmaceutical and food industries. Organic dyes are commonly toxic, carcinogenic and mutagenic.[1,2] Therefore, the discharge of effluents containing organic dyes into environment may not only affect the transparency and aesthetics of water bodies, but also could threaten the normal living and health of aquatic lives and eventually human beings.[2] During the past decades, removal of organic dyes from contaminated effluents has attracted considerable attention. Among various techniques developed to remove dyes from colored wastewater, adsorption has attracted lots of interests due to its advantages including ease of operation, low cost, and no generation of secondary pollution.[3] Many different materials, such as activated carbon,[4] inorganic nanomaterials,[5-7] polymers,[8] metal organic frameworks,[9] solid waste[10] and clay minerals[11] etc., have been used as adsorbents for the removal of organic dyes from aqueous solutions. However, researchers have never stopped to develop novel types of adsorbent materials with higher adsorption capacity, more efficient adsorption performance, and better recycling and reuse properties.

Graphene is a single layer of carbon atoms tightly packed into a two-dimensional honeycomb sp^2 carbon lattice. Due to its extraordinary merits such as high surface area and strong mechanical, thermal and electrical properties, graphene has attracted tremendous research interests. Graphene oxide (GO) is functionalized graphene material with varying oxygen-containing groups (e.g. hydroxyl, epoxide, carboxyl and carbonyl groups). Graphene and GO have been widely studied for adsorptive removal of different environmental pollutants including organic dyes, antibiotics and heavy metals through π-π and electrostatic interactions.[12] However, some drawbacks hinder the direct use of graphene and GO as adsorbents. Serious agglomeration and restacking of graphene sheets can occur during application, which generally results in a great loss of effective surface area and consequently poor adsorption performance. Also, the separation of nanosized graphene- or GO-based adsorbents from aqueous solution through filtration and centrifugation is difficult.[12]

Deposition of different types of inorganic nanoparticles on graphene/GO sheets can impart new functionality to the two-dimensional carbon nanomaterials.[13] Magnetite nanoparticle, which is easy to prepare and demonstrates good biocompatibility, low toxicity, strong superparamagnetism and peroxidase-like activity, has been widely studied and applied in fields like sensors, separation and drug delivery etc.[14] During the past few years, the preparation of magnetic graphene-

[a] Key Laboratory of Industrial Ecology and Environmental Engineering, Ministry of Education, School of Environmental Science and Technology, Dalian University of Technology, Dalian 116024, China. E-mail: shewanella@yahoo.com (Jiti Zhou); Tel./fax: +86 411 84706252.
[b] State Key Laboratory of Urban Water Resource and Environment, Harbin Institute of Technology, Harbin 150090, China. E-mail: waj0578@hit.edu.cn (Aijie Wang); Tel./fax: +86 451 86282195.

based adsorbents via the formation of magnetite nanoparticle and graphene/GO composites has received more attention. The presence of magnetite nanoparticles on graphene sheets can alleviate or avoid the serious agglomeration and restacking of graphene sheets, thus offering more available surface area and higher adsorption capacity. Moreover, magnetic separation of Fe_3O_4-functionalized adsorbents by applying external magnetic field requires less energy and is much easier and more efficient than conventional methods.[15]

Currently, magnetic graphene materials are generally fabricated through chemical coprecipitation,[16-18] hydrothermal or solvothermal reaction,[19-21] and covalent bonding.[22] These approaches usually require the use of toxic reductants and proceed under rigorous conditions (e.g. high temperature and extremely high pH values). To lower the negative impacts on environment, more eco-friendly method for the preparation of magnetite and graphene composites is needed.

It is well known that dissimilatory iron reducing bacteria like *Shewanella* and *Geobacter* species can biologically transform iron oxyhydroxides such as ferrihydrite, goethite, akaganeite and lepidocrocite to magnetite nanoparticles under normal growing conditions.[23,24] Scaled-up production of biogenic magnetite nanoparticles has been carried out.[23] On the other hand, recent studies found that many microbial strains can utilize GO as respiration substrate and efficiently transform it to reduced GO (rGO) in their culture media.[25,26] To the best of our knowledge, no attempt has been conducted to apply microbial cells to fabricate magnetic graphene nanocomposites.

In this paper, we present a simple and eco-friendly approach for preparing magnetite/rGO (MRGO) nanocomposite via successive bioreduction of GO and ferrihydrite by cells of *Shewanella oneidensis* MR-1. The resultant nanocomposite was characterized by transmission electron microscopy (TEM), X-ray diffraction (XRD), Fourier transform infrared spectroscopy (FTIR), X-ray photoelectron spectroscopy (XPS) and vibrating sample magnetometer (VSM). The adsorption properties of the nanocomposite toward organic dyes including methylene blue (MB), malachite green (MG) and crystal violet (CV) were investigated. In addition, separation of the adsorbent by external magnetic field, oxidation of organic dye and regeneration of the adsorbent through Fenton-like reaction, and recycling use of MRGO in repeated adsorption were also conducted.

Experimental Section

Chemicals and bacterial strain

Graphite powder, $Fe(NO_3)_3 \cdot 9H_2O$ and organic dyes including MB, MG and CV were purchased from Sigma-Aldrich or Sinopharm. Graphite oxide was prepared from graphite powder through modified Hummer's method.[27] The aqueous graphite oxide solution was then sonicated for 3 h to facilitate the exfoliation of stacked graphite oxide sheets into mono- or few-layered GO sheets. All other chemicals were of analytical grade and used as received.

Shewanella oneidensis MR-1 was purchased from American Typical Culture Center (ATCC 700550). It was routinely cultured in Luria–Bertani (LB) broth medium at 303 K under aerobic conditions.

Preparation of ferrihydrite

Ferrihydrite precursor was synthesized according to previously described method.[28] Briefly, 1 M KOH was slowly added into 0.1 M $Fe(NO_3)_3 \cdot 9H_2O$ solution under stirring conditions until the pH reached 7.0. The suspension was washed thrice with Milli-Q water (20-30 mL, 18.2 MΩ·cm) and then resuspended in Milli-Q water followed by N_2-flushing (20 min) and anaerobic capping.

Synthesis of MRGO

The biological synthesis route of MRGO is shown in Fig. 1. MR-1 cells cultured overnight in LB medium were harvested through centrifugation (10,000 × g, 5 min), washed thrice with and resuspended in sterile piperazine-N,N′-bis(2-ethanesulfonic acid) (PIPES) buffer (10 mL, 20 mM, pH 7.0). The harvested cell suspensions were then held in anaerobic chamber before use in the following studies. The biopreparation systems were 100 mL serum bottles containing initially 50 mL deoxygenated sterile PIPES buffer, 0.5 g L^{-1} GO and 20 mM lactate supplemented as electron donor. After inoculation of MR-1 cell (1.36 g L^{-1}), the serum bottles were transferred to an incubator shaker (303 K and 150 rpm) and incubated for 12 h. When the color of the solution in the serum bottles changed from brown to black, which indicated the partial reduction of GO by MR-1, freshly-prepared ferrihydrite was supplemented into the systems with a final concentration of 50 mM. The mixture was stirred for 12 h on a magnetic stirrer. After being settled for 12 h, it was stirred again for another 12 h. The incubation was continued until the detection of magnetism of materials in the serum bottles by external magnetic field. The formed materials were separated through external magnetic field, washed thrice with N_2-flushed ultrapure water to remove broth medium and residual bacteria, and then kept as aqueous suspension in an anoxic glovebox before characterization. Microbially reduced GO and biosynthesized magnetite were also similarly prepared using *S. oneidensis* MR-1 without the addition of ferrihydrite and GO, respectively.

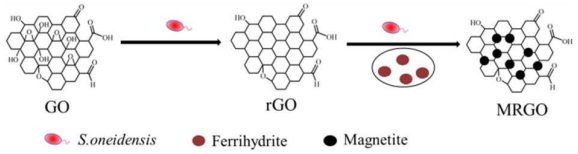

Fig. 1 Synthesis route of MRGO.

Adsorption experiments

All batch adsorption experiments were performed in 100 mL glass bottles containing 30 mL of dye solution on a mechanical shaker at 150 rpm. If not mentioned otherwise, the pH, temperature, initial dye concentration, contact time and adsorbent dosage for adsorption experiments were generally set at 6.0, 303 K, 30 mg L^{-1}, 40 min, and 0.17 g L^{-1}, respectively. Initially, the adsorption properties of MRGO, biogenic rGO and magnetite were compared for the removal of 10-60 mg L^{-1} MB. To investigate the effects of adsorbent dosage, a known amount of MRGO nanocomposite (2.5-12.5 mg) was added to 30 mg L^{-1} dye solutions. The adsorption performance of MRGO for different concentrations of MB was studied via adding 5 mg of MRGO into MB solution of desired initial concentrations (10-60 mg L^{-1}). To study the effects of pH and ionic strength, the initial pH values of the dye solution ranging from 4.0 to 10.0 were adjusted with 0.1 M NaOH or HCl, and the NaCl concentration in the aqueous solution was varied between 0 and 1.0 M, respectively. The effects of temperature on MB adsorption by MRGO were studied with adsorption isotherms at 303, 313 and 323 K.

After magnetic decantation using a permanent magnet, the equilibrium concentrations of dyes were measured with a UV-vis spectrophotometer at maximum absorbance of MB (665 nm), MG (618 nm) and CV (596 nm), respectively. The adsorption capacity (q_e, mg g^{-1}) and removal efficiency (E, %) were calculated based on the difference of dye concentration in aqueous solution before and after adsorption, according to the following equations:

$$q_e = (C_0-C_e)V/m \quad (1)$$

$$E = (C_0-C_e)/C_0\times100\% \quad (2)$$

where C_0 and C_e represent the initial and equilibrium dye concentration (mg L^{-1}), respectively. V and m are the volume of dye solution (L) and the weight of MRGO added (mg), respectively.

All adsorption experiments were performed at least three times. Statistical significance was assessed by one-way ANOVA, and p values less than 0.05 were considered significant.

Peroxidase-like activity of MRGO and regeneration of adsorbent

To test the peroxidase-like activity of biogenic MRGO, both H_2O_2 (5 mL, 30%) and MRGO (10 mg) were added into 30 mL MB solution (10 mg L^{-1}), which was then incubated in a shaker (150 rpm). The oxidation and removal of aqueous MB was determined by measuring the total organic carbon (TOC) concentration of the solution at intervals. The hydroxyl radical generated during this process was detected by electron spin resonance (ESR, JES-FA) with the help of 5, 5-dimethyl-1-pyrroline-N-oxide (DMPO) as the spin trapping agent. DMPO can convert reactive hydroxyl radicals into relatively stable and ESR-detectable nitroxide radicals (spin trap adducts).[29] Control experiments were also conducted with systems containing MRGO or H_2O_2 alone.

The regeneration of MRGO after adsorption was performed through a heterogeneous Fenton-like reaction. Briefly, 10 mg MRGO that reached adsorption equilibrium with MB (10 mg L^{-1}) was collected by external magnetic field, dispersed in 5 mL 30% H_2O_2 and oscillated for 40 min. After that, MRGO was magnetically harvested, washed thrice with 20-30 mL deionized water and then reused in next round of MB adsorption. In total, five rounds of regeneration and reuse were conducted.

Characterization of MRGO

The BET specific surface area of MRGO was determined from N_2 adsorption at –196 °C using a surface area analyzer (Quantachrome NOVA4200e). The morphology and size of MRGO were characterized by TEM with Tecnai G2 spirit transmission electronic microscope operating at 120 kV. XRD analyses of ferrihydrite, GO and MRGO were performed with a Rigaku D/max 2400 X-ray diffractometer (CuKα radiation, k = 0.1541 nm). FTIR spectra of GO and MRGO were recorded by a Bruker Equinox 55 FTIR spectrometer over the wavenumber range of 4000–400 cm^{-1}. Electronic binding energies of GO and MRGO were measured using Thermo Scientific K-Alpha XPS. XPS peaks were deconvoluted by using Gaussian components after a Tougaard background subtraction. The magnetization curve of MRGO was measured with a JDM-13 VSM.

Results and discussion

Characterization of MRGO

As described before, the yellow-brown GO solution turned black in 12 h after inoculation of MR-1, indicating the formation of rGO.[25,26] Then ferrihydrite was added into the serum bottles for further incubation. The color of the mixture turned from brown to black again in the following 4-5 days and the formation of magnetic product was detected by external magnetic field.

In the absence of GO, MR-1 could transform ferrihydrite into clustered and aggregated magnetite nanoparitcles (Fig. S1). On the other hand, as shown in Fig. 2a and b, when ferrihydrite reduction was carried out in the presence of rGO, the iron oxide nanoparticles with an average size of 11.0 nm (Fig. S2) were disorderly distributed on the surface of rGO sheet. The nanoparticles agglomerated in some area of rGO surface due to the dipolar interaction among them. And the BET surface area of MRGO was determined to be 81.7 m^2 g^{-1}.

The XRD patterns of GO, ferrihydrite and MRGO were presented in Fig. 2c. GO displayed diffraction peak at 2ϑ=11.2° corresponding to the (002) plane of GO nanosheets. For MRGO, the peaks at 2ϑ values of 30.3°, 35.8°, 43.5°, 54.3°, 57.5° and 63.1° were assigned to (220), (331), (400), (422), (511) and (440) reflections of cubic spinel crystal structure of Fe_3O_4, respectively. The average grain size estimated from the Fe_3O_4 (331) peak using the Debye Scherrer formula was 10.3 nm, which was in agreement with the mean particle size observed by TEM analysis. In addition, the peak at 23.4° was attributed to (002) reflection of graphene, indicating the coexistence of magnetite and graphene in the nanocomposite.

FTIR spectra of GO and MRGO were shown in Fig. 2d. For GO, the bands at 3180, 1730, 1620, 1240 and 1053 cm^{-1} were attributed to the stretching vibration of O-H, C=O, C=C, C-OH and deformation vibration of C-O. The intensities of peaks relative to oxidized groups decreased evidently in the FTIR spectra of MRGO, indicating the partial reduction of GO by MR-1 cells. Moreover, a new peak at 582 cm^{-1} corresponding to stretching vibration of Fe-O corroborated the presence of magnetite in the nanocomposite.

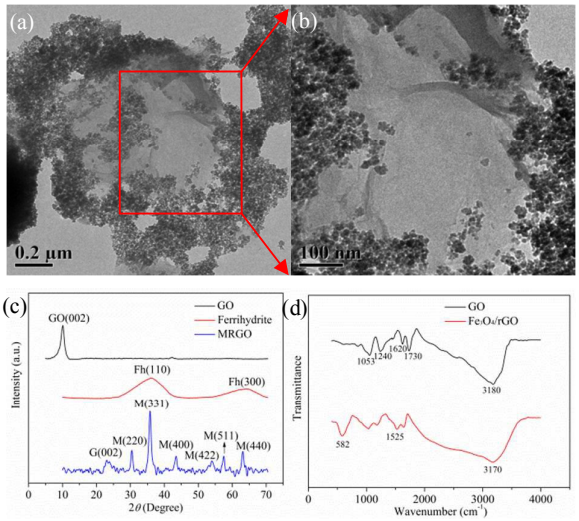

Fig. 2 Characterization of MRGO and its synthesis precursors. TEM of MRGO (a, b), XRD spectra of ferrihydrite, GO and MRGO (c), and FTIR spectra of GO and MRGO (d). Fh, ferrihydrite; G, graphene; M, magnetite.

The chemical states of elements in GO and MRGO were further investigated by XPS (Fig. 3). The sharp peaks in the full scan spectra confirmed the presence of C, O and Fe in MRGO. The four different peaks at 284.5, 286.5, 287.8 and 288.7 eV were assigned to C=C/C-C in aromatic rings, C-O, C=O and O-C=O groups, respectively. The intensities of all the C 1s peaks of the carbons binding to oxygen decreased remarkably, suggesting that most of the oxygen-containing groups were removed through microbial reduction. In the Fe 2p spectra, the peaks at 712.1 and 725.3 eV corresponded to Fe $2p_{3/2}$ and Fe $2p_{1/2}$, respectively. The disappearance of charge transfer satellite of Fe $2p_{3/2}$ at around 720 eV indicated the formation of mixed oxides of Fe(II) and Fe(III) such as magnetite in MRGO.

The magnetic property of MRGO was studied with VSM (Fig. S3). The saturation magnetization of MRGO was determined to be 29.6 emu g^{-1}, which is higher than that (16.3 emu g^{-1}) required for magnetic separation from aqueous solution with a conventional magnet[30] and ensures successful recovery after adsorption in the presence of external magnetic field.

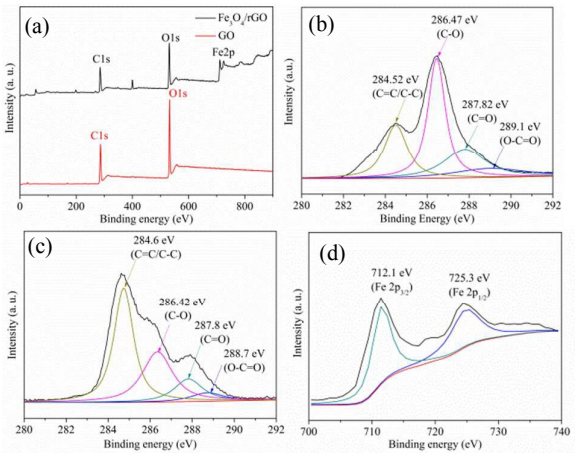

Fig. 3 XPS spectra of MRGO and GO. Wide scan (a), C 1s spectra of GO (b), C 1s spectra of MRGO (c) and Fe 2p spectra of MRGO (d).

Adsorption of MB by MRGO, biosynthesized rGO and magnetite

No removal of MB was observed without the addition of adsorbent (data not shown). As shown in Fig. S4, poor adsorptive removal was observed with microbially synthesized magnetite. Similar removal efficiencies were observed with MRGO and rGO when the concentration of MB was not higher than 20 mg L^{-1}. The removal percentages of rGO were 10-20% higher than those of MRGO when the MB concentration ranged between 30 and 60 mg L^{-1}. The decreased adsorption performance of MRGO might be due to the loss of adsorption sites, which were occupied by magnetite nanoparticles. However, considering MRGO's easy and rapid separation and reclamation, its detailed adsorption performance deserved further investigation.

Effects of MRGO dosage

As shown in Fig. 4, the removal of the three different dyes we studied generally increased with the increase of adsorbent dosage. Almost complete removal of 30 mg L^{-1} MB was achieved in 40 min when the dosage of MRGO was higher than 0.25 g L^{-1}. For CV, the removal efficiency increased from 45.8% to 91.9% when the dosage increased from 0.13 to 0.67 g L^{-1}. An increase of MRGO dosage from 0.1 to 0.5 g L^{-1} resulted in increase of MG removal efficiency from 17.0% to 70.7%.

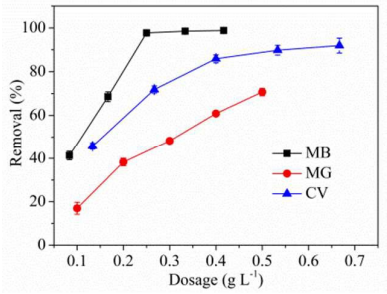

Fig. 4 Effects of MRGO dosage on adsorption removal of MB, MG and CV. C_0 = 30 mg L^{-1}; pH = 6.0; Contact time: 40 min.

Influences of initial pH and ionic strength

No dye precipitation and removal without the presence of MRGO occurred in the pH range we investigated. Relatively poor adsorption (with removal efficiencies less than 47.3%, 19.3% and 28.3% for MB, MG and CV, respectively) was observed when solution pH was lower than 6, whereas abrupt increases in removal efficiencies of the three dyes were observed when the initial solution pH was increased to values higher than 6 (Fig. 5). The point of zero charge (pH_{pzc}) of MRGO was determined to be ~5.3 (Fig. S5). Thus the surface of MRGO was positively charged when $pH<pH_{pzc}$, and negatively charged when $pH>pH_{pzc}$. Therefore, when pH>5.3, the electrostatic attraction force between negatively charged MRGO and cationic dyes significantly improved the adsorptive removal performance. As shown in Table S1, MRGO's dye removal properties under different pH conditions were generally comparable to those of other chemically synthesized magnetic graphene-based adsorbents.

In contrast to the significant influence of solution pH, ionic strength demonstrated limited effects on MB adsorption by MRGO (Fig. 6). For 10 mg L^{-1} MB, the variation of NaCl concentration from 0 to 1 M had almost no influence on the adsorptive removal of MB. For 30 and 50 mg L^{-1} MB, an increase of NaCl concentration to 0.1 M resulted in ~14% decrease of the removal efficiency. A further increase of the NaCl concentration to 1 M led to very limited decrease of the adsorption removal performance. The electrostatic protection that caused by the addition of NaCl could inhibit the electrostatic interaction between adsorbate and adsorbent. Sodium cations at concentrations higher than 0.1 M might compete with positively charged MB for some binding sites on MRGO. Previous studies on MB adsorption by GO-based adsorbent also showed inhibition of adsorption in the presence of higher ion strength (Table S2).

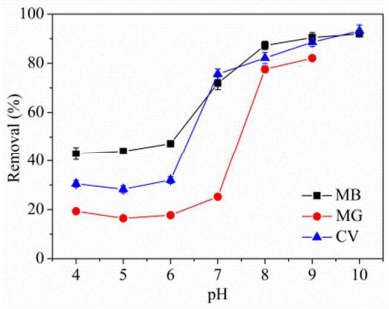

Fig. 5 Effects of initial pH on adsorption removal of MB, MG and CV by MRGO. C_0 = 30 mg L^{-1}; Contact time: 40 min; MRGO dosage: 0.17, 0.2 and 0.3 g L^{-1} for MB, MG and CV, respectively.

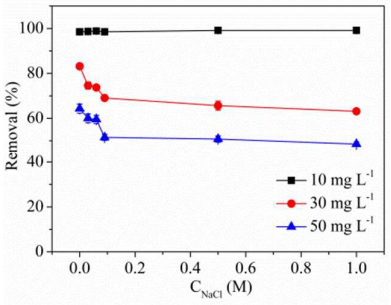

Fig. 6 Effects of ionic strength on adsorption removal of MB by MRGO. C_0 = 10, 30 and 50 mg L^{-1}; Contact time: 40 min; MRGO dosage: 0.17 g L^{-1}; pH = 6.0.

Adsorption isotherms

Adsorption isotherms are useful to understand the adsorption mechanism, surface properties and affinity of the adsorbent towards certain adsorbate, and can provide important information for optimizing the application of adsorbents. Two typical isotherm models, i. e. Langmuir and Freundlich isotherms were employed to describe the adsorption of MB by MRGO at 303, 313 and 323 K. The two isotherm models are expressed as follows:

$$C_e/q_e = 1/(K_L q_{max}) + C_e/q_{max} \quad (3)$$

$$\ln q_e = \ln K_F + 1/n \ln C_e \quad (4)$$

where C_e is the equilibrium concentration of MB in the supernatant (mg L^{-1}); q_{max} is the maximum adsorption capacity of MB per weight of MRGO (mg g^{-1}); K_L represents the Langmuir constant reflecting the affinity of binding sites and energy of adsorption (L mg^{-1}); K_F is the Freundlich constant ($L^{1/n}$ $mg^{1-1/n}$ g^{-1}) indicating the relative adsorption capacity of the adsorbent; $1/n$ is a measure of adsorption intensity. The MB adsorption isotherms at different temperatures were shown in Fig. 7. The Langmuir and Freundlich parameters and the calculated coefficients were summarized in Table 1.The values of regression coefficient (R^2) obtained with the Langmuir model were generally higher than those of Freundlich model. Thus the Langmuir isotherm fits better with the experimental data. And the adsorption of MB onto MRGO is monolayer coverage. It was generally found that dye adsorption by magnetic graphene-based adsorbents at different temperatures were better fitted by the Langmuir isotherm.[18,19,20] The value of the Langmuir equilibrium constant (K_L) increased with increasing temperature, which suggested an increased affinity of MB toward MRGO surface at higher temperature. On the other hand, a dimensionless separation factor (R_L) is generally used to describe whether the adsorption is favorable. The values of R_L suggest irreversible equilibrium (R_L=0), favorable equilibrium (0<R_L<1), linear case (R_L=1) and unfavorable equilibrium (R_L>1), respectively.[31] R_L can be calculated according to the following equation:

$$R_L = 1/(1+K_L C_0) \quad (5)$$

where C_0 is the initial MB concentration. The values of R_L here were determined to be between 0 and 1 at all the tested temperatures (Table 1), indicating that the Langmuir isotherm was favorable under the studied conditions. As shown in Table

2, the maximum adsorption capacity of biogenic MRGO for MB was comparable to or even higher than those of other chemically synthesized magnetite and graphene/GO nanocomposites.

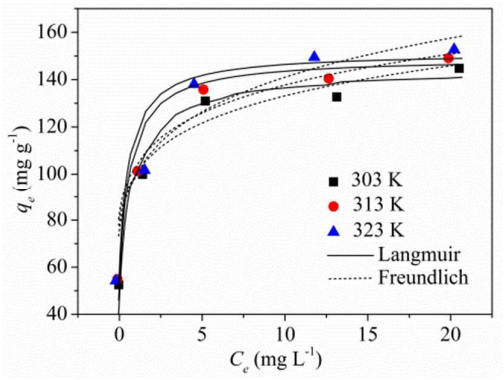

Fig. 7 Langmuir and Freundlich isotherm models for MB adsorption by MRGO at different temperatures. C_0 = 10-50 mg L^{-1}; Contact time: 40 min; MRGO Dosage: 0.17 g L^{-1}; pH = 6.0.

Table 1 Langmuir and Freundlich isotherm parameters.

Model	Parameters	Temperature (K)		
		303	313	323
Langmuir isotherm	q_{max} (mg g^{-1})	144.9	149.3	151.5
	K_L (L mg^{-1})	1.9	2.2	2.5
	R_L	0.01	0.0089	0.0078
	R^2	0.9959	0.9955	0.9928
Freundlich isotherm	*1/n*	0.1337	0.1331	0.1626
	K_F (L$^{1/n}$ mg$^{1-1/n}$ g^{-1})	96.3	99.8	95.1
	R^2	0.9798	0.9981	0.9274

Table 2 Maximum adsorption capacity (q_{max}) values for MB adsorption by various magnetic graphene-based adsorbents.

Adsorbent	Preparation method	q_{max} (mg g^{-1}) /temperature (K)	Refs.
Fe_3O_4/SiO_2-GO	covalent bonding	97.0-111.1/298-333	[32]
Fe_3O_4-chitosan/GO	covalent bonding	95.16/303	[33]
graphene/Fe_3O_4	hydrothermal	43.82/298	[19]
Fe_3O_4@graphene	coprecipitation	45.27/298	[18]
Fe_3O_4/GO	coprecipitation	64.23/298	[16]
β-cyclodextrin-chitosan/GO	covalent bonding	84.32/298	[34]
graphene-Fe_3O_4@carbon	hydrothermal	73.26/298	[20]
Fe_3O_4-GO	covalent bonding	167.2/298	[22]
MRGO	microbial reduction	144.9-151.2/303-323	This study

Kinetic analysis

The time profile of adsorption of different concentrations of MB (10-50 mg L^{-1}) by MRGO was shown in Fig. 8. Fast adsorption process of various concentrations of MB occurred within the first 10 minutes. In addition, the adsorption capacity increased with the increase of initial MB concentration. Higher driving force that generated by higher initial MB concentration could more effectively overcome the mass transfer resistance and lead to more collisions between MB molecules and active sites on MRGO.

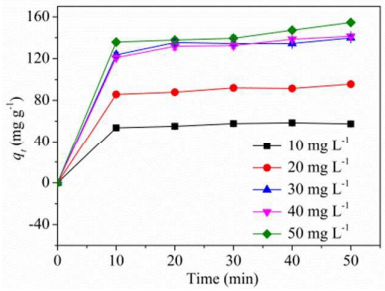

Fig. 8 Effects of adsorption time on removal of MB by MRGO. C_0 = 10-50 mg L^{-1}; MRGO dosage: 0.17 g L^{-1}; pH = 6.0.

To further understand the adsorption mechanism, two different kinds of kinetic models were applied to study the kinetics of MB adsorption on MRGO. The pseudo-first-order and pseudo-second-order kinetic models are expressed as follows:

$\log(q_e-q_t) = \log q_e - k_1 t/2.303$ (6)

$t/q_t = 1/(k_2 q_e^2) + t/q_e$ (7)

where q_e and q_t are the amount of MB adsorbed per unit mass of MRGO (mg g^{-1}) at equilibrium and time t, respectively. k_1 (min^{-1}) and k_2 (g mg^{-1} min^{-1}) represent the pseudo-first-order and pseudo-second-order kinetic constant, respectively. The kinetic parameters obtained through linear regression for the two models were shown in Table 3. It was obvious that the correlation coefficient (R^2) values of the pseudo-second-order model were higher than those of pseudo-first-order. And the calculated q_e values ($q_{e,\ cal}$) from the pseudo-second-order model agreed better with the experimental data ($q_{e,\ exp}$). Thus the adsorption kinetics of MB by MRGO followed the pseudo-second-order model. The kinetics of MB adsorption by other magnetic graphene-based adsorbents were also better described with pseudo-second-order model.[19,34,35] The decrease of k_2 with the increase of initial MB concentration might be due to the longer time required to reach the equilibrium state. Moreover, the values of initial adsorption rate v_0 (mg g^{-1} min^{-1}) determined by the following equation:

$v_0 = k_2 q_e^2$ (8)

were also shown in Table 3. The values of v_0 here are higher than those of other studies,[32,36] indicating the good MB adsorption properties of MRGO at initial stage.

Thermodynamic study

The thermodynamic study is helpful for understanding the inherent energetic variation during the adsorption process. Different thermodynamic parameters, including the Gibb's free energy (ΔG^0), enthalpy (ΔH^0) and entropy (ΔS^0) were calculated according to the following equations:

$\Delta G^0 = -RT\ln K_d$ (9)

$\ln(K_d) = \Delta S^0/R - \Delta H^0/RT$ (10)

where K_d is the distribution coefficient ($K_d = q_e/C_e$), T is the temperature (K) and R is the gas constant (8.314 J mol^{-1} K^{-1}).

As shown in Table 4, the ΔG^0 values were negative at tested temperatures, indicating that the adsorption of MB to MRGO was a spontaneous process. The ΔG^0 value became more negative with the increase of temperature, suggesting that higher temperature could facilitate the adsorption. The positive value of ΔH^0 indicated an endothermic nature of the adsorption. In general, adsorption process with a ΔG^0 value between 0 and −20 kJ mol^{-1} is believed to be physisorption, while adsorption process with a ΔG^0 value between −80 and −400 kJ mol^{-1} is suggested to be chemisorption.[37] Kara et al.[38] reported that the ΔH^0 of physisorption is generally smaller than 40 kJ mol^{-1}. Therefore, the calculated values of ΔG^0 and ΔH^0 here suggested that the MB adsorption by MRGRO is a physisorption process. And the positive value of ΔS^0 revealed that the randomness at the solid/solution interface increased during the adsorption process.

Regeneration through Fenton-like reaction

Peroxidase-like activity has recently been found with magnetite nanoparticle and magnetite/GO nanocomposite, which could function as catalyst of heterogeneous Fenton-like reaction and promote the decomposition of H_2O_2 to hydroxyl radical.[14,35] The peroxidase-like activity of biogenic MRGO and generation of hydroxyl radicals were firstly confirmed by time-course ESR measurements using DMPO as spin trap. As shown in Fig. S6, in the presence of MRGO, the ESR signal displayed an intense four-peak spectrum with an intensity ratio of 1:2:2:1, which is the typical and characteristic ESR signal of DMPO-·OH and suggests that H_2O_2 is activated by MRGO to hydroxyl radicals. The intensity of the signal increased as time went on during the monitored period of 60 min. For control experiments, no hydroxyl radical was detected with system containing MRGO alone without H_2O_2. And the background hydroxyl radical concentration of H_2O_2 remained at a low level throughout the investigation without the addition of MRGO (data not shown).

After treatment of MB solution with MRGO and H_2O_2, no color was observed with the final solution. Decreasing TOC of the solution (Fig. S7) indicates that MB molecules were oxidized by hydroxyl radicals. Repeated use in multiple runs is important for regenerated magnetic adsorbent. Traditionally, adsorbate on the adsorbent is eliminated through washing with organic solvents or calcining at high temperatures, which is time-/energy-consuming and may cause secondary pollution. The identification of peroxidase-like activity with MRGO provided a new approach for the oxidative removal of adsorbed molecules and regeneration of magnetic graphene adsorbents. The MRGO regenerated by Fenton-like reaction demonstrated stable adsorption performance during repeated usage. Removal of over 70% MB (10 mg L^{-1}) could be achieved in successive four runs of operation and removal efficiency of around 60% could still be achieved in the fifth run (Fig. 9). Generally, the loss and aggregation of MRGO nanocomposites during regeneration and recycling processes might be responsible for the decrease of adsorption properties after repeated operations. In addition, some adsorbed dye molecules that cannot be removed by regeneration could occupy the adsorption sites on the surface of the adsorbent, which could also result in declining adsorption performance.[39] Compared to traditional regeneration methods which applied organic solvent or NaOH solution to wash the used graphene-based adsorbent, the regeneration process here applying Fenton-like reaction resulted in comparable or even higher adsorption efficiency after four rounds of repeated usage (Table S3).

Table 3 The values of kinetic parameters obtained by different models.

Mode	Parameters	C_0 (mg L^{-1})				
		10	20	30	40	50
Pseudo-first-order model	k_1 (min^{-1})	0.06	0.034	0.031	0.059	0.029
	$q_{e,cal}$ (mg g^{-1})	8.89	13.49	14.81	37.41	28.29
	$q_{e,exp}$ (mg g^{-1})	58.43	95.59	139.87	141.39	154.56
	R^2	0.7729	0.8017	0.4678	0.9044	0.7906
Pseudo-second-order model	k_2 (g $mg^{-1}min^{-1}$)	0.0125	0.0093	0.0088	0.0027	0.0022
	$q_{e,cal}$ (mg g^{-1})	59.88	95.23	138.89	147.06	158.73
	$q_{e,exp}$ (mg g^{-1})	58.43	95.59	139.87	141.39	154.56
	v_0 (mg g^{-1} min^{-1})	44.82	84.34	169.76	58.39	55.43
	R^2	0.9997	0.9972	0.9978	0.999	0.9947

Table 4 Thermodynamic parameters for MB adsorption by MRGO.

T (K)	ΔG^0 (kJ mol^{-1})	ΔH^0 (kJ mol^{-1})	ΔS^0 (J mol^{-1} K^{-1})
303	-12.47	16.14	94.45
313	-13.43		
323	-14.35		

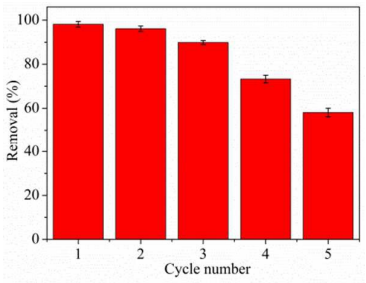

Fig. 9 Reusability of MRGO for MB removal. C_0 = 10 mg L^{-1}; Contact time: 40 min; MRGO dosage: 0.17 g L^{-1}; pH = 6.0.

Conclusions

For the first time, magnetite/reduced graphene oxide nanocomposite was biologically prepared with culture of *S. oneidensis* MR-1 and shown to be effective for adsorption of organic dyes. The adsorption of MB by the biogenic nanocomposite can be satisfactorily described by Langmuir isotherm and pseudo-second-order kinetic model, and is a spontaneous and endothermic process. Moreover, after magnetic decantation with external magnetic field, the adsorbent could be regenerated through Fenton-like reaction and showed good reusability in successive operations. This study shows an environment-friendly way to fabricate reusable graphene-based adsorbent. The biogenic nanocomposite can be used as a new platform for the decontamination of organic dyes and other pollutants in aqueous solution. Moreover, considering that microbes possess diverse metabolism activities and can produce many other different metal/metalloid (oxides) nanomaterials under normal growing conditions, it would be interesting to explore the eco-friendly fabrication of other graphene-based nanocomposites with microbial cells.

Acknowledgements

This work was supported by National Natural Science Foundation of China (No. 51478076) and Open Project of State Key Laboratory of Urban Water Resource and Environment, Harbin Institute of Technology (No. QAK201530).

References

1 K. Hunger, *Industrial Dyes: Chemistry, Properties, Applications*, Wiley-VCH, Weinheim, 2003.
2 R. M. Christie, *Environmental Aspects of Textile Dyeing*, Woodhead Publishing, Cambridge, 2007.
3 M. T. Yagub, T. K. Sen, S. Afroze, H. M. Ang, *Adv. Colloid Interface Sci.*, 2014, **209**, 172–184.
4 S. Karagöz, T. Tay, S. Ucar, M. Erdem, *Bioresour. Technol.*, 2008, **99**, 6214–6222.
5 J. Fan, W. Cai, J. Yu, Chem-Asian J., 2011, **6**, 2481–2490.
6 Y. Yao, F. Xu, M. Chen, Z. Xu, Z. Zhu, *Bioresour. Technol.*, 2010, **101**, 3040–3046.
7 P. Z. Ray, H. J. Shipley, *RSC Adv.*, 2015, **5**, 29885-29907.
8 Y. Tang, T. Hu, Y. Zeng, Q. Zhou, Y. Peng, *RSC Adv.*, 2015, **5**, 3757–3766.
9 D. Liu, Z. Xie, L. Ma, W. Lin, *Inorg. Chem.*, 2010, **49**, 9107–9109.

10 L. C. Oliveira, M. Gonçalves, D. Q. Oliveira, M. C. Guerreiro, L. R. Guilherme, R. M. Dallago, *J. Hazard. Mater.*, 2007, **141**, 344–347.
11 E. Errais, J. Duplay, M. Elhabiri, M. Khodja, R. Ocampo, R. Baltenweck-Guyot, F. Darragi, *Colloids Surf. A Physicochem. Eng. Asp.*, 2012, **403**, 69–78.
12 G. Z. Kyzas, E. A. Deliyanni, K. A. Matis, *J. Chem. Technol. Biotechnol.*, 2014, **89**, 196–205.
13 P. T. Yin, S. Shah, M. Chhowalla, K. B. Lee, *Chem. Rev.*, 2015, **115**, 2483–2531.
14 L. Gao, J. Zhuang, L. Nie, J. Zhang, Y. Zhang, N. Gu, T. Wang, J. Feng, D. Yang, S. Perrett, X. Yan, *Nat. Nanotechnol.*, 2007, **2**, 577–583.
15 R. Sivashankar, A. B. Sathya, K. Vasantharaj, V. Sivasubramanian, *Environ. Nanotechnol. Monit. Manage.*, 2014, **1–2**, 36–49.
16 J. H. Deng, X. R. Zhang, G. M. Zeng, J. L. Gong, Q. Y. Niu, J. Liang, *Chem. Eng. J.*, 2013, **226**, 189–200.
17 J. Chen, Y. Hao, Y. Liu, J. Gou, RSC Adv., 2013, **3**, 7254-7258.
18 Y. Yao, S. Miao, S. Liu, L. P. Ma, H. Sun, S. Wang, *Chem. Eng. J.*, 2012, **184**, 326–332.
19 L. Ai, C. Zhang, Z. Chen, *J. Hazard. Mater.*, 2011, **192**, 1515–1524.
20 W. Fan, W. Gao, C. Zhang, W. W. Tjiu, J. Pan, T. Liu, *J. Mater. Chem.*, 2012, **22**, 25108–25115.
21 W. Wang, T. Jiao, Q. Zhang, X. Luo, J. Hu, Y. Chen, Q. Peng, X. Yan, B. Li, *RSC Adv.*, 2015, **5**, 56279-56285.
22 G. Xie, P. Xi, H. Liu, F. Chen, L. Huang, Y. Shi, F. Hou, Z. Zeng, C. Shao, J. Wang, *J. Mater. Chem.*, 2012, **22**, 1033–1039.
23 J. M. Byrne, H. Muhamadali, V. S. Coker, J. Cooper, J. R. Lloyd, *J. R. Soc. Interface*, 2015, **12**, 20150240.
24 T. Perez-Gonzalez, C. Jimenez-Lopez, A. L. Neal, F. Rull-Perez, A. Rodriguez-Navarro, A. Fernandez-Vivas, E. Iañez-Pareja, *Geochim. Cosmochim. Acta.*, 2010, **74**, 967–979.
25 G. Liu, X. Zhang, J. Zhou, A. Wang, J. Wang, R. Jin, H. Lv, *Bioresour. Technol.*, 2013, **149**, 503−508.
26 G. Wang, F. Qian, C. W. Saltikov, Y. Jiao, Y. Li, *Nano Res.*, 2011, **4**, 563−570.
27 W. S. Hummers Jr, R. E. Offeman, *J. Am. Chem. Soc.*, 1958, **80**, 1339–1339.
28 R. M. Cornell, U. Schwertmann, *The Iron Oxides: Structure, Properties, Reactions, Occurences and Uses*, Wiley-VCH, Weinheim, 2003.
29 Y. Lei, C. S. Chen, Y. J. Tu, Y. H. Huang, H. Zhang, *Environ. Sci. Technol.*, 2015, **49**, 6838–6845.
30 Z. Y. Ma, Y. P. Guan, H. Z. Liu, *J. Polym. Sci. Pol. Chem.*, 2005, **43**, 3433–3439.
31 K. R. Hall, L. C. Eagletow, A. Acrivers, T. Vermeulen, *Ind. Eng. Chem. Res.*, 1966, **5**, 212–218.
32 Y. Yao, S. Miao, S. Yu, L. P. Ma, H. Sun, S. Wang, *J. Colloid Interface Sci.*, 2012, **379**, 20–26.
33 L. Fan, C. Luo, X. Li, F. Lu, H. Qiu, M. Sun, *J. Hazard. Mater.*, 2012, **215–216**, 272–279.
34 L. Fan, C. Luo, M. Sun, H. Qiu, X. Li, *Colloids Surf. B Biointerfaces*, 2013, **103**, 601–607.
35 N. A. Zubir, C. Yacou, J. Motuzas, X. Zhang, J. C. Diniz da Costa, *Sci. Rep.*, 2014, **4**, 4594.
36 H. Sun, L. Cao, L. Lu, *Nano Res.*, 2011, **4**, 550–562.
37 C. Weng, Y. Lin, T. Tzeng, *J. Hazard. Mater.*, 2009, **170**, 417–424.
38 M. Kara, H. Yuzer, E. Sabah, M.S. Celik, *Water Res.*, 2003, **37**, 224–232.
39 H. Wang, H. Jiang, S. Wang, W. Shi, J. He, H. Liu, Y. Huang, *RSC Adv.*, 2014, **4**, 45809–45815.

Microbial preparation of magnetite/reduced graphene oxide nanocomposite for removal of organic dyes from aqueous solutions

Guangfei Liu,[a, b] Ning Wang, [a] Jiti Zhou,[*a] Aijie Wang,[*b] Jing Wang,[a] Ruofei Jin,[a] Hong Lv[a]

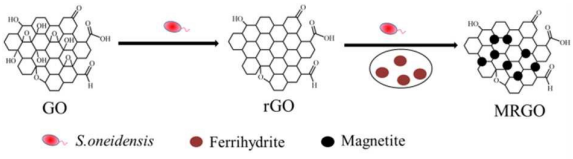

Magnetite/rGO nanocomposite synthesized by microbial cells can function as effective dye adsorbent and be regenerated through Fenton-like reaction.